A Study of the 3D Unmanned Remote Surveying for the Curved Semi-Shield Tunneling

Jinyi Lee*, and Jongwoo Jun**

*Department of Information, Control and Instruments, Chosun University, Gwangju, Korea
(Tel : +82-62-230-7101; E-mail: jinyilee@chosun.ac.kr)
** Eon Solution, Pusan, Korea
(Tel : +82-51-610-0061; E-mail: eon@eonsnd.com)

Abstract: Semi-shield tunneling is one of the propulsion construction methods used to lay pipes underground between two pits named 'entrance' and 'destination', respectively. Usually a simple composition, such as 'a fiducial target at the entrance+a total station (TS)+a target on the machine', is used to confirm the planned course. However, unavoidable curved sections are present in small-sized pipe lines, which are laid after implementation of a road system, for public works such as waterworks, sewer, electrical power, and gas and communication networks. Therefore, if the planned course has a curved section, it is difficult to survey the course with the abovementioned simple composition. This difficulty could be solved by using the multiple total stations (MTS), which attaches the cross type linear LED target to oneself. The MTS are disposed to where each TS can detect the LED target at the other TS or the base point or the machine. And the accurate relative positions between each MTS and target are calculated from measured data. This research proposes the relative and absolute coordinate calculation algorithm by using three MTS to measure a curved course with 20m curvature at 30m maximum distance, and verifies the algorithm experimentally.

Keywords: remote surveying, semi-shield tunneling, total station, planned course, coordinate calculation

1. INTRODUCTION

Semi-shield tunneling is one of the propulsion construction methods used to lay pipes underground between two pits named 'entrance' and 'destination', respectively. A tunneling machine digs under ground, and an oil pressure jack in the entrance pushes the tunneling machine and the pipes following the machine. The operator drives the machine to the top, bottom, left and right sides remotely towards the destination pit. This semi-shield tunneling is useful for small size tunneling of under 2000mm diameter, and has merits such as minimizing the ground displacement, traffic obstructions, and environmental damages, reducing work period because of the high propulsion speed, overcoming spatial limitation in a downtown area because it needs only two pits on the road [1~4].

Generally, the small-sized pipe lines for public goods such as waterworks, sewer, electrical power, and gas and communication networks are laid after implementation of a road system in the city. Therefore, the curved sections of the pipe lines are unavoidable because of the road system of the city. It is important to develop an unmanned remote surveying system for semi-shield tunneling, which must be carried out in dangerous surveying environment such as small space, impure air, electric shock, and fear. Also, such a system would reduce the surveying time and term of work, minimize the errors between the planned path and digging path, and expand the distance between the pits.

We investigate 3-dimensional unmanned remote surveying for curved semi-shield tunneling by using the reported optical distance data and angle measurement devices[5,6] (hereafter TS, total station). Cross-type linear LED, which can be controlled remotely, is attached to the tunneling machine and positioned at the entrance base point. The TS is composed of a photo diode circuit to generate a signal when the linear LED light is inserted into the visual angle of the optical system, the motorized stages moves to rotate the electro-optical system to the 3-axis angle, a laser range finder tracks to measure the distance, the CCD linear sensors and optical components operate to measure the accurate angles between the machine base point and the center of crossed LED light. Also this electro-optical device is maintained to the absolute horizon by using a motorized automatic stage system. Each TS is fixed to internal of the semi-shield pipes, finds the cross type linear LED targets automatically, and calculates the present position of the machine from the fiducial point at the entrance.

But if the planned course has a curved section, it is difficult to survey the course with this simple composition, 'a target at the entrance-a TS-a target on the machine', because the TS's viewing angle is hided by the curved wall. This difficulty could be solved using the multiple TS (hereafter MTS), which attaches the cross type linear LED target to itself. The MTSs are disposed to where each TS can detect the LED target at the other TS or at the base point and the machine. And the accurate relative positions of the each MTS and targets are calculated from measured data. We propose the absolute coordinate calculation algorithm by using the developed three MTS to measure a curved course and verify the algorithm experimentally.

2. PRINCIPLES AND POSITION CALCULATION ALGORITHM

2.1 Remote auto-tracking distance and angle measurement system

Remote auto-tracking distance and angle measurement system (hereafter TS, total station) is fixed in the pipe to measure the angle and distance from a fiducial point of the entrance to a tunneling machine. Fig. 1 shows a photograph of a developed and reported TS [5,6]. A rotation stage (b) and a goniometer (c) are fixed on an automatic optical bread board system (a). A sensor device system and a laser range finder (d) on the stages to measure the angle and the distance could be rotated vertically or horizontally. Also TS can be controlled by using each control part (hereafter SB, station box, (e)). The SB controls the automatic optical bread board system, the rotate stage, the goniometer, the laser range finder, the photo sensor and the CCD linear sensor by computer command through communication connector. By using a TS and an SB, two targets, which are positioned at the toward and backward, can be detected automatically, and the angle and the distance from the TS fiducial point can be measured. On the other hand, a telescope of the TS has a 2.5-degree viewing angle. A photo sensor and two CCD linear sensors are positioned on the extension line of the optical center of the telescope. Also the

telescope and the laser range finder are parallel on their optical center line.

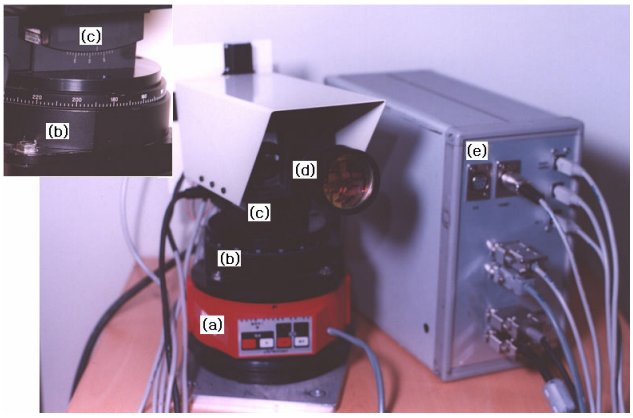

Fig. 1 A trial total station.

2.2 Targets

Fig.2 shows a target positioned at the entrance. A 3-D unmanned remote surveying system for the curved semi-shield tunneling uses a target positioned at the entrance to measure and calculate the present absolute coordinate of the tunneling machine as shown in Fig. 2. Also the absolute coordinates of the each TS and the tunneling machine can be measured and calculated using the shows targets as shown in Fig. 3 which are positioned at the back of the TS and the tunneling machine, respectively.

All of the targets are controlled by abovementioned SB. The center of the target can be searched at high speed because the sufficiently large line type LED light is inputted to the viewing angle of the telescope. Also the target has a large area, from which the light of laser range finder can be reflected. On the other hand, the horizontal or vertical direction LED on the target could be turned on or off selectively with electrical signal from the SB.

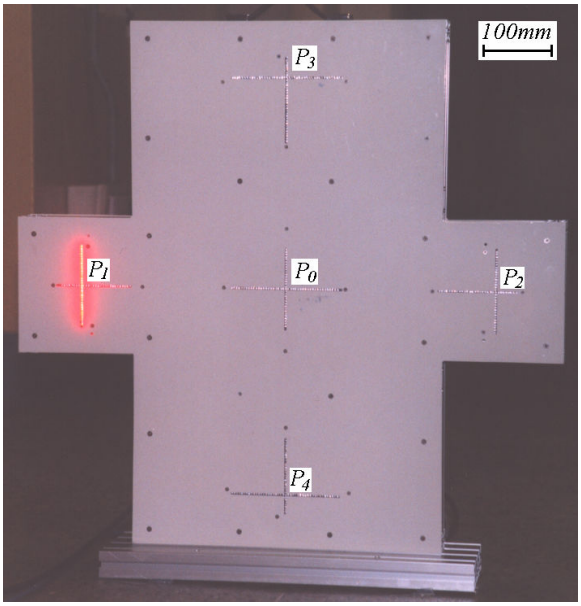

Fig. 2 Target positioned at the entrance.

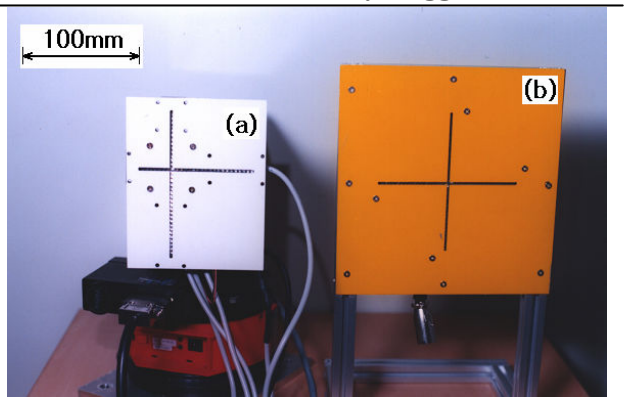

Fig. 3 Target for auto tracking (a) target positioned back of te each TS (b) target positioned at the tunneling machine.

2.3 Precision angle measurement

The motorized rotate stage encoder and the goniometer encoder have the high accuracies such as 0.0025 degrees and 0.0008 degrees, respectively. However the real angular accuracies cannot exceed ± 1.0 degrees because the photo sensor response when the LED light is inputted to the viewing angle of the telescope and the rotate stage stop after the response. Actually these low angular accuracies induce the very large errors on the surveying results. Therefore the high precision angle measurement method using the CCD linear sensors (hereafter CLS) were developed and reported [5, 6]. A CLS(Sony, ILX554B) has 2048 arrayed photo sensors with the $14\mu m \times 56\mu m$ size and the $14\mu m$ intervals. The center position where the maximum optical intensity is inputted can be calculated using the principle shown in Fig. 4. If the line type LED light is inputted to the viewing angle of the telescope as shown in Fig. 4(a), the optical intensity and the 8-bits digitized optical voltages are distributed as shown in Fig. 4 (b) and (c), respectively. The Y_C and Y_i mean the center positions in the maximum optical voltage distribution at where the LED light is positioned at the exact center of the telescope viewing angle and at where the LED light is positioned at the certain position of the telescope viewing angle, respectively. Therefore, the CLS pixel which express Y_C is always decided. But the Y_i pixel is various because the rotate stage would be stopped certainly when the LED light is inputted to the viewing angle. The number of pixels from Y_C to Y_i , ΔY_i can be calculated using Eq. (1).

$$\Delta Y_i = \frac{N+M}{2} - Y_C \qquad (1)$$

The M and N are the boundary pixels which are under the certain critical optical intensity determined at the CLS electrical circuits. Fig. 5 shows an example of the distribution of the digitized optical intensity on the CLS and the calculation of the Y_i. If the digitized critical intensity is 32, the M and N are 810 and 867, respectively. And the center position Y_i is to be 838.5 in this case. Considering the line type LED light on the target were out of the telescope viewing angle when the rotate stage or the goniometer rotate the angle of θ_1. This LED light is positioned in the viewing angle when the rotate angle is θ_2. Also the LED light is located in the viewing angle continuously when the rotate angle is θ_3, θ_4 after rotating a

certain angle $\Delta\theta$ and $2\Delta\theta$. The exact center angle which the LED light is positioned at the exact center of the viewing angle, θ_C can be derived using Eq. (2) [5, 6].

$$\theta_C = \theta_3 + \frac{\Delta\theta}{\Delta Y} \cdot \left[\frac{\Delta Y_2 + \Delta Y_3 + \Delta Y_4}{3} \right] \quad (2)$$

Where, ΔY_2, ΔY_3 and ΔY_4 are the number of pixels from the center of CLS to the each optical intensity center positions when the rotate angles are θ_2, θ_3 and θ_4. The $\Delta\theta / \Delta Y$ is the angle per unit pixel, and is characteristics of each TS.

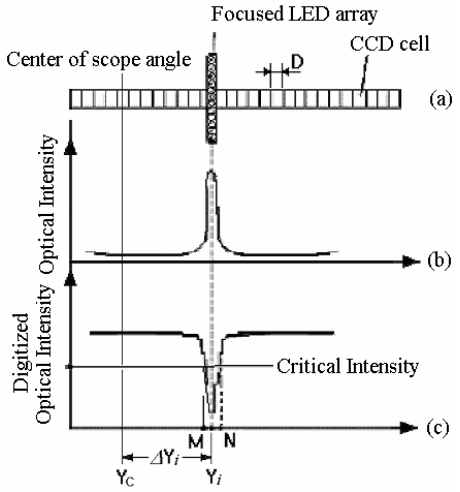

Fig. 4 Principles of CCD linear sensor

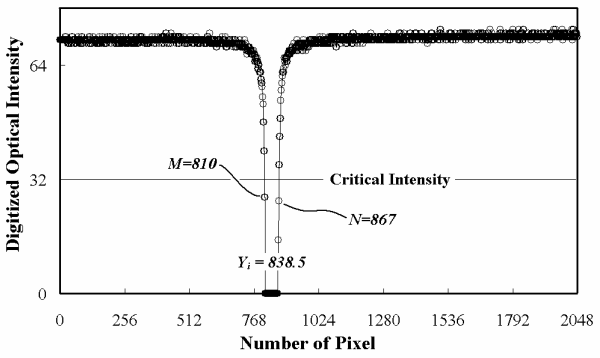

Fig. 5 Distribution of intensity on the CLS.

2.4 Coordinate system and position calculation algorithm

P_0, Y, and XY plane mean the fiducial point at the entrance, the initial propulsion direction, and the absolute horizontal plane, respectively, as shown in Fig.6 and Fig.7. Z axis passes through the P_0 in a vertical direction to the XY plane. P_1 and P_2 are positioned at the distance Δx and –Δx to the X direction from the P_0. And P_3 and P_4 are positioned at the distance Δz and –Δz to the Z direction from the P_0. The center points of 4-pair cross type LED are expressed as P_1(Δx, 0, 0), P_2(-Δx, 0, 0), P_3(0 ,0, Δz) and P_4(0, 0, -Δz). T(x, y, z) is the mechanical center of TS. And B(x_1, y_1, 0) and D(0, y_1, z_1) are the projecting planes of T(x, y, z) to the XY and YZ plane, respectively. A(x_1, 0, 0) and C(0, y_1, 0) are the projecting lines of B(x_1, y_1, 0) to the X and Y axis. E(x_1, 0, -Δz), F(x_1, y_1, -Δz), G(0, y_1, -Δz) and H(0, 0, -Δz) are points on the projection plane which is parallel to the XY plane and passes through P_4(0, 0, -Δz). L_{1P1}, L_{1P2} and L_{1P4} express the distances from T(x_1, y_1, z_1) to P_1(Δx, 0, 0), P_2(-Δx, 0, 0) and P_4(0, 0, -Δz), respectively. Also, L_{1P1}', L_{1P2}' and L_{1P4}' express the projection distances of the L_{1P1}, L_{1P2}, L_{1P4} to the XY plane. Furthermore, L_{1P1}'', L_{1P2}'' and L_{1P4}'' express the projection distances of the L_{1P1}, L_{1P2}, L_{1P4} to the YZ plane. These projection distances can be expressed as follows in Eq. (3).

$$\begin{vmatrix} L_{1P1}' & L_{1P2}' & L_{1P4}' \\ L_{1P1}'' & L_{1P2}'' & L_{1P4}'' \\ L_{1P1} & L_{1P2} & L_{1P4} \end{vmatrix} = \begin{vmatrix} \overline{TP_1} & \overline{TP_2} & \overline{TP_4} \\ \overline{BP_1} & \overline{BP_2} & \overline{BP_0} \\ \overline{TA} & \overline{TA} & \overline{TE} \end{vmatrix} \quad (3)$$

Fig. 7 show the projection planes of the 3D coordinate system, as shown in Fig.6, to the XY (Fig.7(a)) and the YZ plane(Fig.7(b)). The optical system on the rotation stage turns toward the certain direction of the digging course. Where α_{T1}^{P0}, α_{T1}^{P1} and α_{T1}^{P2} are the angles from the certain direction to P_0, P_1 and P_2, respectively, and it was purchased using the CCD linear sensors and the precise angle calculation methods [5, 6]. Also, β_{T1}^{P1}, β_{T1}^{P2}, β_{T1}^{P4}, the angles from the absolute horizon to the $\overline{DP_1}$, $\overline{DP_2}$, $\overline{DP_4}$, are easily calculated using these methods [5] because the TS can be maintained the absolute horizon by using the automatic optical bread board system. Correspondingly, the present absolute coordinate of TS, (x_1, y_1, z_1) can be calculated using Eq. (4) and Eq. (5).

$$\begin{aligned} x_1 &= \frac{1}{4\Delta x}\left({L'_{1P2}}^2 - {L'_{1P1}}^2 \right) \\ y_1 &= \sqrt{{L'_{1P2}}^2 - (\Delta x - x_1)^2} \\ z_1 &= -L_{1P4} \cdot \sin\beta_{T1}^{P4} - \Delta z \end{aligned} \quad (4)$$

$$\text{where, } \begin{aligned} L'_{1P1} &= L_{1P1} \cdot \cos\beta_{T1}^{P1} \\ L'_{1P2} &= L_{1P1} \cdot \cos\beta_{T1}^{P2} \end{aligned} \quad (5)$$

Similarly, the 3 dimensional locations of the each TS and the target of the tunneling machine (hereafter TM) as shown in Fig.7 can be expressed as follows:

$$\begin{aligned} x_2 &= x_1 + L'_{12} \cdot \sin\alpha_1 \\ y_2 &= y_1 + L'_{12} \cdot \cos\alpha_1 \\ z_2 &= z_1 + L''_{12} \cdot \sin\beta_{T2}^{T1} \end{aligned} \quad (6)$$

$$\begin{aligned} x_3 &= x_2 + L'_{23} \cdot \sin\alpha_2 \\ y_3 &= y_2 + L'_{23} \cdot \cos\alpha_2 \\ z_3 &= z_2 + L''_{23} \cdot \sin\beta_{T3}^{T2} \end{aligned} \quad (7)$$

$$\begin{aligned} x_4 &= x_3 + L'_{3TM} \cdot \sin\alpha_3 \\ y_4 &= y_3 + L'_{3TM} \cdot \cos\alpha_3 \\ z_4 &= z_3 + L''_{3TM} \cdot \sin\beta_{T3}^{TM} \end{aligned} \quad (8)$$

$$\text{where, } \begin{aligned} \alpha_1 &= \alpha_{T1}^{P2} + \cos^{-1}\left(\frac{y_1}{L'_{1P2}} \right) - \pi - \alpha_{T1}^{T2} \\ \alpha_2 &= \alpha_{T2}^{T1} - \pi - \alpha_{T2}^{T3} \\ \alpha_3 &= \alpha_{T3}^{T2} - \pi - \alpha_{T3}^{TM} \end{aligned} \quad (9)$$

$$
\begin{aligned}
L'_{12} &= L_{12} \cdot \cos \beta_{T1}^{T2} \\
L''_{12} &= L_{12} \cdot \cos \alpha_1 \\
\text{and} \quad L'_{23} &= L_{23} \cdot \cos \beta_{T2}^{T3} \qquad (10) \\
L''_{23} &= L_{23} \cdot \cos \alpha_2 \\
L'_{3TM} &= L_{3TM} \cdot \cos \beta_{T3}^{TM} \\
L''_{3TM} &= L_{3TM} \cdot \cos \alpha_3
\end{aligned}
$$

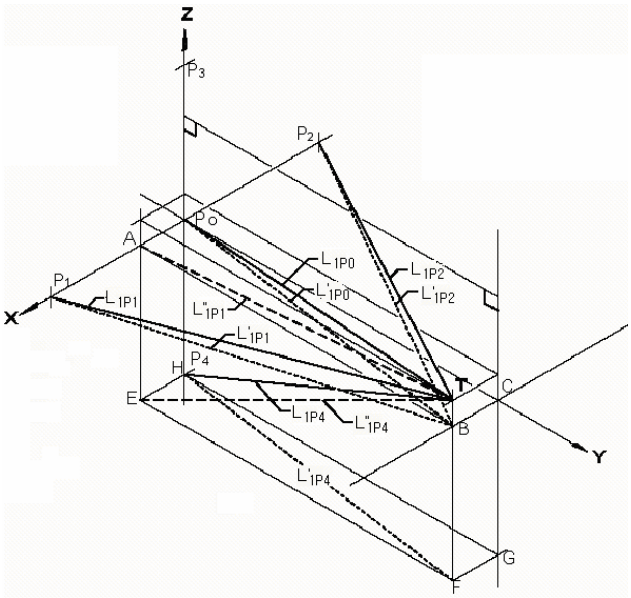

Fig. 6 Coordinate system of tunneling

3. EXPERIMENTS AND DISCUSSIONS

The repetition accuracies of the each TS were examined for all fixed locations of TS. The locations of the TSs are in the following order: the main target (hereafter MT) at the entrance, followed by TS1, TS2, TS3 and a target (hereafter TM) on the tunneling machine as shown in Fig. 7. As such, 3 cases of locations were considered: (1) MT-TS3-TM, (2) MT-TS2-TS3-TM, and (3) MT-TS1-TS2-TS3-TM. Each TS had a target on the back. Correspondingly, the 3 cases as shown in Table 1 were examined to consider the repetition accuracies of the each TS. The examined and calculated results using Eqs. (3) ~ (10) showed repetitions of x_{Error}= 2.27~68.96mm, y_{Error}=0.15~1.00mm and z_{Error}=0.26~2.54mm in this case. The repetitions of y and z direction were under 2.54mm at the maximum distance of 37.93m; so, each TS has error of under 0.0038 degrees and very high precision. But the repetition in the x direction was about 70mm.

Table 1 Repetition when TS are fixed on fixed location.

(units: mm)

Items	x_1	y_1	z_1	x_2	y_2	z_2
Main target + TS3 + Target	574.57	18150	294.88	782.14	27384	252.19
	543.88	18151	296.40	766.76	27385	254.73
	574.57	18150	294.88	782.14	27384	252.19
Errors	30.69	1.00	1.51	15.38	1.00	2.54
Main target + TS2 + Target(TS3)	-472.60	18934	363.22	223.75	37931	368.58
	-508.03	18932	363.48	153.39	37931	370.43
	-507.23	18932	363.22	154.79	37930	370.17
Errors	34.63	1.00	0.26	68.96	1.00	1.85
Main target + TS1 + Target(TS2)	-492.54	11833	140.97	-508.06	24464	253.65
	-490.43	11834	139.63	-503.27	24464	251.59
	-490.27	11834	141.01	-502.81	24463	252.97
Errors	2.27	0.15	1.38	5.24	1.00	2.07

A horizontal angle, α_{T1}^{P2}, a vertical angle, β_{T2}^{T1} and the distance, L_{1P1} and L_{12} were considered in Eqs. (3) ~ (10) to investigate the low repetition accuracy at the x direction value. Various values of α_{T1}^{P2} were calculated as shown in Table 2. The x position at the TM, x_2, was affected mainly by the change in α_{T1}^{P2}. But the real mechanical accuracy of the TS horizontal angle was under 0.0025 degrees, so x_2 had 0.0035mm of repetition accuracy, as shown in Table 2. This repetition value meant that the horizontal angle of TS such as α_{T1}^{P2} could not have been the cause of the low repetition in this MTS system.

Table 2 Calculated repetition accuracy when the α_{T1}^{P2} is changed.

(units: mm)

No.	α_{T1}^{P2}	x_1	y_1	z_1	x_2	y_2	z_2
1	1972255	-381.58	12092	-135.13	-438.38	20051	-180.62
2	1973255	-381.58	12092	-135.13	-452.27	20051	-180.62
3	1974255	-381.58	12092	-135.13	-466.16	20050	-180.62
4	1975255	-381.58	12092	-135.13	-480.05	20050	-180.62
5	1976255	-381.58	12092	-135.13	-493.94	20050	-180.62
Errors	0.1 degrees increasing	0.00	0.00	0.00	13.89	0.16	0.00
Mech. errors	0.0025 degrees	0.00	0.00	0.00	0.0035	0.399 x10^{-4}	0.00

On the other hand, Table 3 shows the calculated results when the vertical angle β_{T2}^{T1} was changed at 0.01 intervals. It shows that the z position at the TM, z_2, was affected mainly by of the change of β_{T2}^{T1}. But the real mechanical accuracy of the TS vertical angle was under 0.008 degrees, so z_2 had about 1.4mm of repetition accuracy as shown in Table 3. This repetition value meant that the vertical angle of TS such as β_{T2}^{T1} could not have been the cause of the abovementioned low repetition in this MTS system.

Table 3 Calculated repetition accuracy when the β_{T2}^{T1} is changed.

(units: mm)

No.	β_{T2}^{T1}	x_1	y_1	z_1	x_2	y_2	z_2
1	-0.3075	-381.58	12092	-135.13	-466.16	20050	-177.85
2	-0.3175	-381.58	12092	-135.13	-466.16	20050	-179.24
3	-0.3275	-381.58	12092	-135.13	-466.16	20050	-180.63
4	-0.3375	-381.58	12092	-135.13	-466.16	20050	-182.01
5	-0.3475	-381.58	12092	-135.13	-466.16	20050	-183.40
Errors	0.01 degrees increase.	0.00	0.00	0.00	0.00	0.01	1.39
Mech. errors	0.008 degrees	0.00	0.00	0.00	0.00	0.01	1.38

The calculated results showed that the x positions were strongly affected when the distances L_{1P1} and L_{12} changed at 1mm intervals, respectively, as shown in Table 4. Furthermore, the real mechanical accuracy of the TS laser range finder was ±1.5mm, so the abovementioned low repetitions were due to the distance measurement error.

Table 5 shows the experimental results in the curved micro semi-shield tunneling simulation course by the 3 MTS system. The first item, 'MT+TS3+TM', means the initial state: A TS was positioned between an MT and a TM. The second item, 'MT+TS2(Add)+TS3+TM', means that the TS2 was added to the above state between the MT and the TS1.

Table 4 Calculated repetition accuracy when the L_{1P1} and L_{12} were changed. (units: mm)

No.	L_{1P1}	L_{12}	x_1	y_1	z_1	x_2	y_2	z_2
1	12095	7961	-341.34	12094	-135.13	-399.44	20053	-180.61
2	12094	7960	-361.46	12093	-135.13	-432.80	20052	-180.62
3	12093	7959	-381.58	12092	-135.13	-466.16	20050	-180.63
4	12092	7958	-401.70	12091	-135.13	-499.52	20049	-180.63
5	12091	7957	-421.81	12090	-135.13	-532.88	20048	-180.64
Errors	1mm decr.	1mm decr.	20.12	1.15	0.00	33.36	1.30	0.01

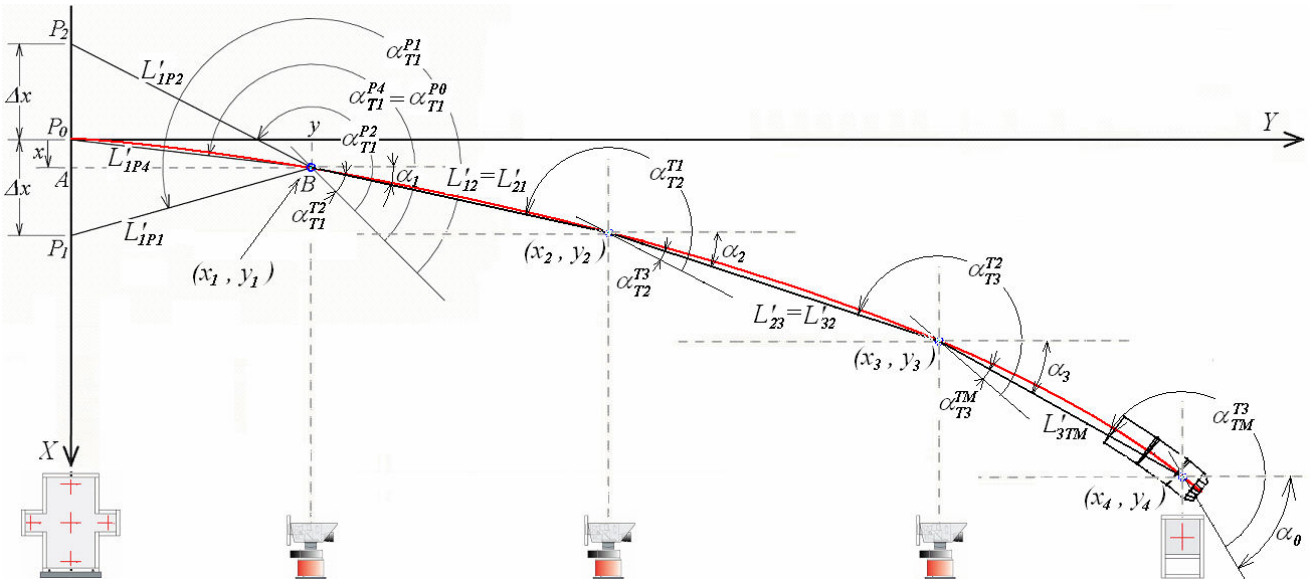

(a) A projecting plane on XY

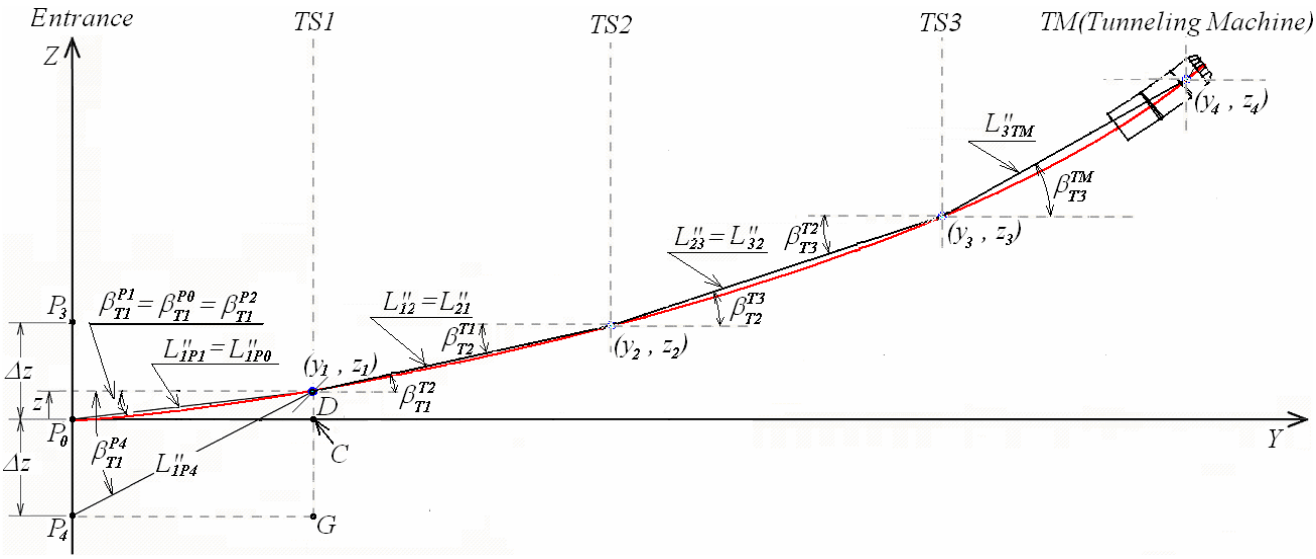

(b) A projecting plane on YZ

Fig. 7 Projections on the XY and YZ planes

Table 5 Experimental results using 3 total stations system.

(units: mm)

Items	x_1	y_1	z_1	x_2	y_2	z_2	x_3	y_3	z_3	x_4	y_4	z_4
MT + TS3 + TM							563.92	18852.72	304.90	796.10	27384.43	258.69
							563.98	18850.67	305.13	795.92	27384.38	257.49
							533.03	18852.09	305.69	778.14	27384.44	259.35
MT + TS2(Add)+ TS3+ TM				102.31	10260.61	168.72	488.84	18851.84	305.21	911.78	27377.22	257.57
Errors							75.14	0.88	0.48	115.59	7.22	1.78
MT + TS2(Move) + TS3 (Move) + TM(Move)				578.26	19379.99	349.28	1901.35	38568.61	362.48	2995.60	47539.91	338.29
				577.25	19380.03	349.25	1905.92	38568.07	362.18	3003.68	47539.13	337.99
				577.89	19380.02	349.58	1898.71	38568.61	361.97	2993.16	47540.07	337.78
MT + TS1(Add) + TS2 + TS3 + TM	140.32	10379.08	220.87	570.81	19376.89	348.13	2418.01	38521.98	358.92	3756.10	47460.35	338.16
	138.03	10379.03	221.16	569.91	19376.78	347.66	2422.81	38520.31	364.88	3763.00	47457.35	340.07
	154.94	10378.28	221.46	602.07	19374.26	350.12	2486.39	38514.72	369.22	3840.51	47451.68	345.78
Errors	16.91	0.80	0.59	24.82	-3.10	1.92	587.68	53.89	3.56	847.35	88.38	0.12

In this case, the maximum errors were 75.14mm and 115.59mm at x_3 and x_4, respectively. These errors were due to the fact that measured distance had a small error at the laser range finder as abovementioned. 'MT+TS2(Move)+TS3 (Move)+TM(Move)" means that the TS2, TS3 and TM moved according to the same simulation course. And 'MT+TS1(Add) +TS2+TS3+TM' means that the TS1 was added to the above state between the MT and the TS2. Similarly, with the case of 'MT+TS2(Add)+TS3+TM', the maximum errors existed at x_1, x_2, x_3 and x_4. Furthermore, the errors in the y positions increased when the total stations were added. These errors accumulated as shown in Eqs. (2) ~ (6). But the errors in the z positions were small and were permitted in the proposed MTS system. Correspondingly, if the laser range finder has a sufficient precision of under mm, the above errors will be ignored and the algorithm using the proposed equations will be useful to calculate the curved course in the micro semi-shield tunneling environment.

4. CONCLUSIONS

The absolute coordinate calculation algorithms using the developed 3 multi-total station systems were proposed to measure a curved course in the micro semi-shield tunneling environment. Each absolute positions of the total stations and the tunneling machine were calculated using the distances examined by the laser range finder and the angles examined by the CCD linear sensor and the telescope optical components on the automatic optical bread board. The repetition accuracies of the each total station were x_{Error}=2.27~68.96mm, y_{Error}=0.15~1.00mm and z_{Error}=0.26 ~2.54mm. The repetitions of y and z direction were under 2.54mm at the maximum distance of 37.93m. These values mean that each total station had under 0.0038 degrees error and very high precision. But the repetition in the x direction was about 70mm. A horizontal angle, a vertical angle, and the distance were considered to investigate the low repetition accuracy. The small distance errors such as ±1.5mm are strongly affected to the x direction repetition accuracy. Correspondingly, if the laser range finder has a sufficient precision of under mm, these errors will be ignored and the proposed algorithm will be useful for the calculation of the curved course in micro semi-shield tunneling environment

REFERENCES

[1] M. Choi, C. Lee and M. Kim, "Present and future of the micro-tunneling techniques", *Korean Geotechnical Society*, Vol.16, No.1, pp.26-33, 2000.

[2] J. Nam, "Automatic course control techniques for the micro-tunneling machines", *Korean Society of Civil Engineeris*, Vol.48, No.10, pp.67-71, 2000.

[3] A. Kohzo, T. Fujimoto, E. Nagano, H. Sasaki, T.Takeuchi, D. Hatsuji, " Development of long span pipe jacking method for laying underground pipe", *Technical report of Kawasaki Steel*, Vol.20, No.1, pp.83-88, 1988.

[4] T. Miyahara, O. Nobe, H. Tanaka, "Development of jacking pipe for pipeline with ultra sharp curve", *Technical report of Kumimoto*, No.41, pp.48-55, 1999.

[5] J.Lee and J. Kim, "Development of auto tracking total station for unmanned remote surveying of micro tunneling with curved courses", *Journal of Control, Automation, and Systems Engineering*, Vol.9, No.11, pp.891-898, 2003.

[6] J. Lee, J. Jeon and J. Nam, "Development of total station for in-line measuring of curved course in micro-tunneling", *Proceedings of IEEK Summer Conference 2003*, Vol.26, No.1, 2003.